



Contents lists available at SciVerse ScienceDirect

Tetrahedron

journal homepage: www.elsevier.com/locate/tet

The origin of stereoselectivity in cycloaddition reactions promoted by stereoisomers of 8-phenylmenthyl glyoxylate oxime

Carlos A.D. Sousa^{a,*}, Carlos F.R.A.C. Lima^a, Mariana Andrade^b, Xerardo García-Mera^c, José E. Rodríguez-Borges^{a,*}

^a Centro de Investigação em Química, Department of Chemistry and Biochemistry, Faculty of Science, University of Porto, Rua do Campo Alegre, 4169-007 Porto, Portugal

^b Centro de Materiais da Universidade do Porto, Rua do Campo Alegre, 4169-007 Porto, Portugal

^c Department of Organic Chemistry, Faculty of Pharmacy, University of Santiago de Compostela, E-15782 Santiago de Compostela, Spain

ARTICLE INFO

Article history:

Received 12 December 2012
Received in revised form 6 March 2013
Accepted 8 March 2013
Available online xxx

Keywords:

8-Phenylmenthyl glyoxylate oximes
Stereoselectivity
Chiral auxiliary
Aza-Diels–Alder
1,3-Cycloaddition
Aromatic interactions

ABSTRACT

A structural study of three synthesized stereoisomeric oximes, (–)-8-phenylmenthyl glyoxylate oxime (8-PMGO), (+)-8-phenylneomenthyl glyoxylate oxime (8-PnMGO), and (–)-8-phenylisoneomenthyl glyoxylate oxime (8-PinMGO), was performed by means of variable temperature ¹H NMR spectroscopy, X-ray crystallography, and ab initio calculations. It was found that in 8-PMGO a conformation where the phenyl and oxime moieties are stacked is significantly favored, whereas in the other stereoisomers this preference was not so evident. The conformational differences found between the isomers were used to rationalize the outcome of the reaction (simultaneous 1,3-cycloaddition and aza-Diels–Alder reaction) between the referred oximes and cyclopentadiene, in which the stereoselectivity was evaluated and found to be nicely reproduced by a simple conformational analysis. The global results indicate that the stereoselectivity of the studied oximes, a bit higher for 8-PMGO, originates from their particular conformational distribution, in which the phenyl-oxime aromatic interaction plays a decisive role.

© 2013 Elsevier Ltd. All rights reserved.

1. Introduction

Since the introduction of 8-phenylmenthol as a chiral auxiliary by Corey,¹ there are not many examples of the usage of its stereoisomers.² Just recently the other 8-phenylmenthol stereoisomers have been used and proved to have potential as chiral auxiliaries in asymmetric synthesis, particularly in aza-Diels–Alder reactions.³

From the time when 8-phenylmenthol started to be used, it exhibited excellent results as chiral auxiliary, leading to high diastereomeric and enantiomeric excesses in asymmetric synthesis,^{1,2,4} this essential feature being considered to be related to its structure.^{1d,5} In solution, even when it is complexed to Lewis acids, the phenyl group of an acrylate ester of 8-phenylmenthol (as an example) is believed to be positioned so as to allow an attractive interaction between the π double bond of the acryloyl group and the aromatic ring, which is well positioned under the acrylic ester π system at a favorable stacked π – π spacing of approximately 3.5 Å.^{1d} As a result of this interaction, the phenyl ring blocks one of the diastereotopic faces of the acrylic ester π system, thus forcing the approach of the reactants from the other side, giving rise to a large

diastereomeric excess. Some computational calculations⁶ and experimental data⁷ seem to sustain this interpretation. In fact, the structures of the compounds obtained from reactions between acrylate esters and dienes (as cyclopentadiene, CPD), in which 8-phenylmenthol is used as chiral auxiliary, as well as the observed diastereoselectivities, are in agreement with the described analysis. Nonetheless, in the cases of aza-Diels–Alder reactions, in which the dienophile is usually an imine, such interpretation is expected to be more complex. Comparatively to acrylates, imines may adopt diverse conformations (e.g., *s-cis/s-trans* and *E/Z* conformations), allowing more possible structures to exist in solution. Moreover, such conformations may be strongly dependent on the reaction conditions as solvent, temperature, presence of a catalyst and on the catalyst itself. Considering this, and also the increase on the application of the other 8-phenylmenthol stereoisomers in asymmetric synthesis, we intended to compare and rationalize the resulting stereoselectivity in cycloaddition reactions when those different stereoisomers are employed as chiral auxiliaries. To do this, (–)-8-phenylmenthyl, (+)-8-phenylneomenthyl, and (–)-8-phenylisoneomenthyl glyoxylate oximes (8-PMGO, 8-PnMGO, and 8-PinMGO, respectively) (Fig. 1) were structurally analyzed in solution, condensed and gas phases; in addition, 8-PMGO and 8-PnMGO were reacted with CPD in order to evaluate their

* Corresponding authors. Fax: +351 220 402 659; e-mail addresses: carlos.sousa@fc.up.pt (C.A.D. Sousa), jrborges@fc.up.pt (J.E. Rodríguez-Borges).

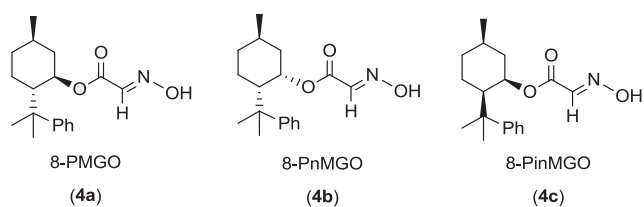


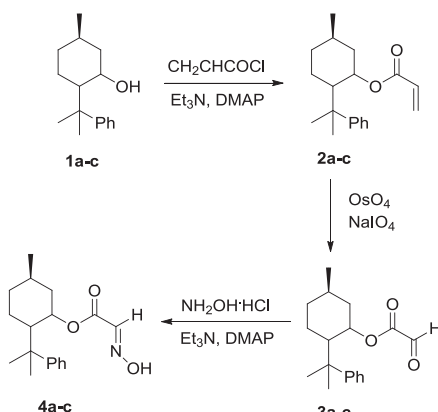
Fig. 1. Structural formulas of the oximes considered in this work, and respective abbreviations.

enantioselectivities by analyzing the obtained cycloadducts (the isoxazolidines being the major products).⁸

2. Results and discussion

2.1. Synthesis

(–)-8-phenylmenthol (**1a**), (+)-8-phenylneomenthol (**1b**), and (–)-8-phenylisoneomenthol (**1c**) were synthesized according to the literature.^{3a} The correspondent acrylates (**2a–c**) were prepared by treatment with acryloyl chloride in the presence of triethylamine. The oxidative cleavage of the acrylate's double bond by $\text{OsO}_4/\text{NaIO}_4$ provided the respective glyoxylates (**3a–c**).^{2,3d} 8-PMGO, 8-PnMGO, and 8-PinMGO (**4a–c**, respectively) were synthesized according to a previously reported method,⁸ from their respective glyoxylates by treatment with hydroxylamine hydrochloride in the presence of triethylamine and a catalytic amount of DMAP (Scheme 1).



Scheme 1. Procedure adopted for the synthesis of the studied oximes.

2.2. Conformational study

For each oxime, ^1H NMR spectra were recorded at several temperatures in CDCl_3 and the chemical shifts (δ) of the more significant protons were plotted against T . All the values were scaled by considering δ at the lower temperature as zero.

The ^1H NMR spectra (see Supplementary data) show that the H_{imine} signal in 8-PMGO (6.79 ppm) has a high upfield shift relative to both 8-PnMGO and 8-PinMGO ($\delta=7.45$ and 7.50 ppm, respectively). This fact suggests the existence of a significant degree of $\pi\cdots\pi$ stacking between the phenyl ring and the glyoxylate oxime π system in 8-PMGO, the upfield shift arising from the shielding effect produced by the magnetic anisotropy of the phenyl ring.⁹ On the other hand, the chemical shifts of the H_{imine} for the other isomers are similar to those of other aliphatic *E* aldioximes,¹⁰ which suggests that no significant $\pi\cdots\pi$ stacking occurs between the

phenyl ring and the glyoxylate oxime moiety in both 8-PnMGO and 8-PinMGO.

The effect of the temperature on the ^1H NMR spectra was also studied. Signals for characteristic protons of the 8-phenylmenthyl moiety for each of the three oximes [$5'\text{-CH}_3$, $2\times 8'\text{-CH}_3$ (represented as a, b, and c, respectively), and $\text{Ph-H}_{\text{para}}$] were monitored, showing negligible changes in the chemical shifts with temperature. Concerning the H_{imine} signals of 8-PnMGO and 8-PinMGO, one can verify that the dependence of their chemical shift with temperature is very small (see Supplementary data). The plot of $\Delta\delta$ against T for 8-PMGO is presented in Fig. 2. In this case a significant downfield shift of the imine proton is observed as the temperature increases, which can be due to thermal displacement from the conformation in which the intramolecular $\pi\cdots\pi$ stacking exists.

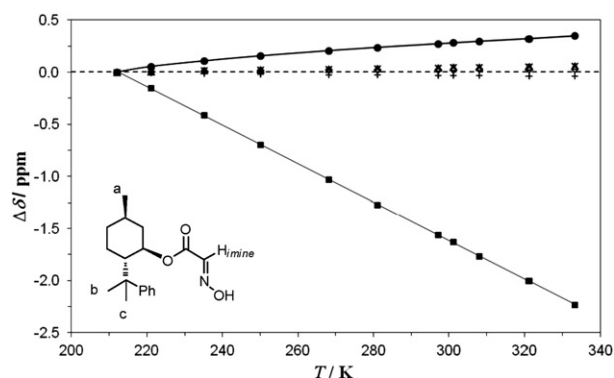


Fig. 2. Temperature dependence of the proton chemical shifts, $\Delta\delta$, in 8-PMGO. Legend: ■ OH; × CH_3 a; Δ CH_3 b; ◇ CH_3 c; + $\text{Ph-H}_{\text{para}}$; ● H_{imine} .

NOEs NMR were also performed for the three oximes. Some NOE effect between H_{imine} and the aryl protons in 8-PMGO was observed. On the contrary, for 8-PnMGO and 8-PinMGO, a small NOE signal was observed between H_{imine} and $8'\text{-CH}_3$ protons while no (or a negligible) NOE signal was detected between H_{imine} and the aryl protons (see Supplementary data for more details).

In summary, the NMR results are consistent with the fact that in 8-PMGO the phenyl ring and the glyoxylate oxime π system establish an intramolecular $\pi\cdots\pi$ interaction; however there are no evidences for this same interaction in 8-PnMGO and 8-PinMGO.

In view of these results we carried out an ab initio computational study in order to better understand the conformational behavior of the studied oximes. The torsional potentials about the dihedral angle, ϕ_1 , depicted in Fig. 3 for 8-PMGO, 8-PnMGO, and 1-(2-cyclohexylpropan-2-yl)benzene were obtained at the SCS-MP2/cc-pVDZ level of theory.¹¹ Since there are conformers able to establish intramolecular aromatic interactions, which involve a large fraction of dispersion forces, the use of a method that accounts for correlation energy is mandatory. SCS-MP2/cc-pVDZ has been employed before to yield fairly accurate results on relatively large aromatic systems with intramolecular aromatic

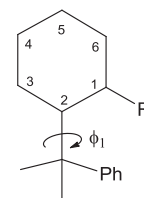


Fig. 3. Schematic representation of the dihedral angle, ϕ_1 , considered for the evaluation of the internal rotation profiles in (2-cyclohexylpropan-2-yl)benzene ($\text{R}=\text{H}$), 8-PMGO, and 8-PnMGO/8-PinMGO ($\text{R}=\text{O}-\text{C}(\text{O})-\text{C}(\text{H})=\text{N}-\text{OH}$).

interactions.¹² In the calculations, the C(R)–C–C–Ph dihedral angle was frozen at regular intervals and the rest of the molecule was allowed to relax. The methyl group in the position C5 of the cyclohexane ring was not considered in the calculations, since its influence in the equilibrium geometries and torsional potentials is expected to be negligible, thus improving the speed of the calculations. Without the methyl group, 8-PnMGO is the enantiomer of 8-PMGO, being molecules energetically not distinguishable. Hence, the calculations for 8-PnMGO also apply to the 8-PinMGO case. The results for the total electronic energies obtained from the optimized structures of the selected compounds, as well as the detailed results for the torsional potential energy profiles, are presented in [Supplementary data](#).

The influence of the *s*-cis/*s*-trans conformation of the imine moiety in the torsional potentials of the titled compounds was estimated by computing the relative energies of the respective conformers for methyl glyoxylate oxime (R'=CH₃ in [Fig. 7](#)) at the B3LYP/6-311++G(d,p) and SCS-MP2/cc-pVDZ levels. Both methods show that the conformers are nearly isoenergetic with a barrier of interconversion of about 20 kJ mol⁻¹ (further details presented as [Supplementary data](#)), which indicates roughly equimolar equilibrium and rapid interconversion between the conformers at ambient temperature. However, from a practical point of view, the extrapolation of the structures of the three oximes in gas phase (or even in solution) for a reaction course must be careful. For example, in a cycloaddition reaction, the presence of an acid catalyst is normally required, which may influence the structure of the oxime. In fact, the addition of an acid catalyst as H⁺, and thus nitrogen protonation, will probably favor the *s*-cis conformer of the imine moiety, since stronger H-bonds in esters commonly involve the carbonyl oxygen instead of the alkoxy group.¹³ This assumption was checked by calculating the relative energies of the nitrogen-protonated *s*-cis/*s*-trans methyl glyoxylate oxime conformers, showing that the *s*-cis isomer is favored by approximately 10 kJ mol⁻¹ (details in [Supplementary data](#)).

Even though a complete structural study should include a full characterization of the torsional profiles in the *s*-trans isomers as well, it is assumed that the *s*-trans profiles will not deviate from the *s*-cis ones in any considerable extent. In this way, the *s*-cis conformers were considered for full characterization of the torsional profiles. The fact that the *s*-cis conformation is the one adopted in the crystal phase of 8-PnMGO also supports our choice (see [Fig. 10](#)). The vibrational degree of freedom corresponding to the C(cyclohexyl)–O bond rotation ([Fig. 5](#)) must also be considered for a full characterization of these systems, since it leads to additional minima in the potential energy surfaces (PES) of 8-PMGO and 8-PnMGO. A quick inspection of [Fig. 5](#) shows that in 8-PnMGO the C2 conformer is substantially less stable than C1; C1 is also the conformation adopted in the crystal phase, further supporting this observation. In this way, conformer C2 was not included in the computational study. However, for 8-PMGO the energetic differentiation is not so obvious and thus the C(R)–C–C–Ph torsional potential was also sketched for the C2 conformation.

The gas phase computational results are, in principle, a good approximation to solution, considering the CDCl₃ solvent used in the VT ¹H NMR experiments, which should not be capable of inducing significant structural changes in 8-PMGO, 8-PnMGO, and

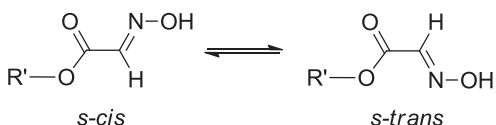


Fig. 4. The *s*-cis/*s*-trans isomerism in the imine moiety of the considered oximes.

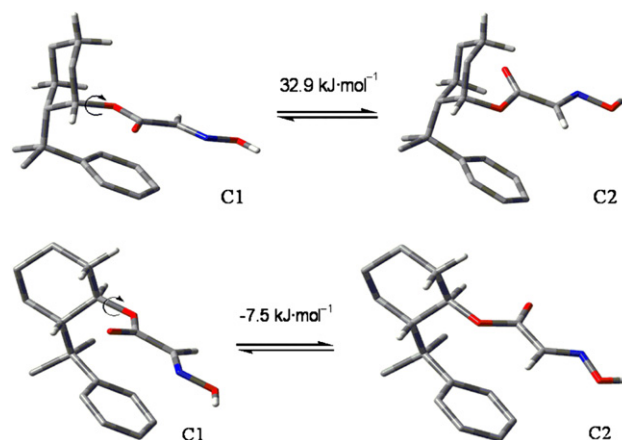


Fig. 5. Rotation about the C(cyclohexane)–O bond leads to other minima in 8-PnMGO (top) and 8-PMGO (bottom). The C2 conformer of 8-PnMGO is substantially less stable than C1. In 8-PMGO the energetic distinction between C1 and C2 is not so obvious, and thus the two conformations will be considered henceforth. Gas phase SCS-MP2/cc-pVDZ result is presented. Some H atoms are omitted for clarity.

8-PinMGO. However, it must be noted that solvation may slightly affect the torsional profiles, since in solution internal rotations are generally more restricted than in the gas phase and CDCl₃ has the ability to establish CH⋯π interactions with aromatic rings.¹⁴ The potential energy profiles for the C(R)–C–C–Ph torsion in the considered compounds are presented in [Figs. 6–8](#).

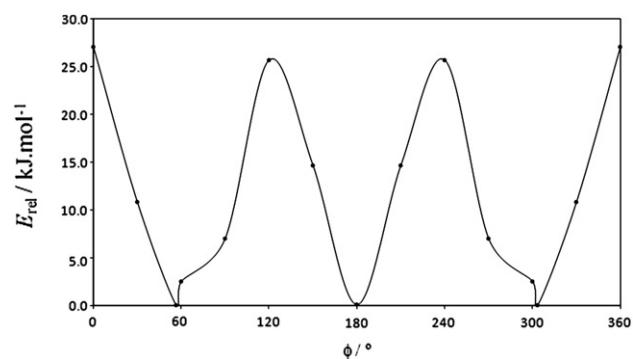


Fig. 6. Potential energy profile for the internal rotation about the C(R)–C–C–Ph dihedral angle for 1-(2-cyclohexylpropan-2-yl)benzene, R=H, at the SCS-MP2/cc-pVDZ level of theory.

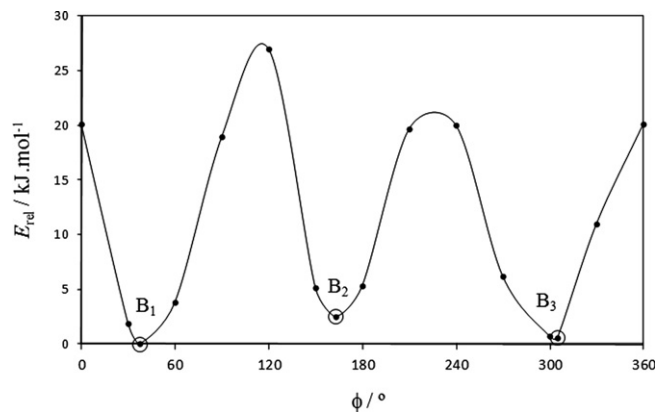


Fig. 7. Potential energy profile for the internal rotation about the C(R)–C–C–Ph dihedral angle for 8-PnMGO and 8-PinMGO at the SCS-MP2/cc-pVDZ level of theory, considering the *s*-cis conformer of the imine moiety.

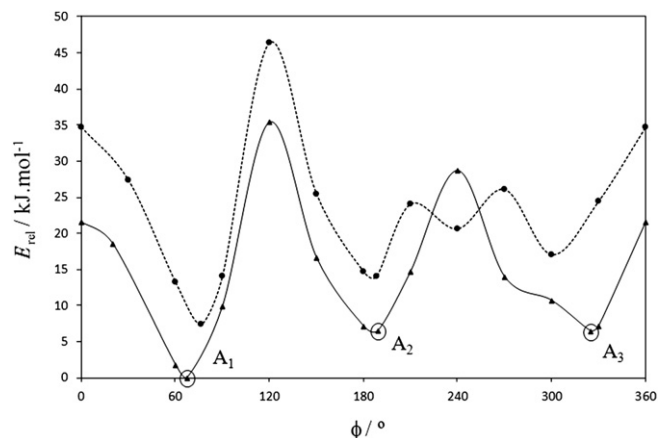


Fig. 8. Potential energy profile for the internal rotation about the C(R)–C–C–Ph dihedral angle for the C1 (●, dotted line) and C2 (▲, full line) conformers of 8-PMGO at the SCS-MP2/cc-pVDZ level of theory, considering the *s*-cis conformer of the imine moiety.

While for 8-PnMGO and 8-PinMGO (Fig. 7) this potential is near symmetric, resembling the (2-cyclohexylpropan-2-yl)benzene case (Fig. 6), for both the C1 and C2 conformers of 8-PMGO (Fig. 8) there is an important asymmetry in the torsional potential that clearly favors the A₁ conformer over A₂ and A₃. As shown in Fig. 9 (top) for the C2 conformer, the relative position of the phenyl group in A₁ is such that the imine proton experiences a significant shielding effect due to the close proximity of the benzene ring current, contributing to the upfield shift observed in NMR. By inspection of Fig. 9 one can see that in A₂ the imine proton is far away from any significant steric effect, indicating that in this conformation the chemical shift of this proton must be very similar to the imine group alone. In contrast, in A₃, the imine proton is in a deshielding region relative to the benzene ring current. In this way, as *T* increases, the molecules will have a lower average population of the A₁ conformer, diluting the shielding effect felt in this conformation, but higher

populations of the A₂ and A₃ conformers, increasing the deshielding effect of the A₃ conformer, the A₂ one having a practically null stereochemical effect on the imine proton chemical shift. The combination of these effects is consistent with the pronounced deshielding of this proton as *T* increases, observed experimentally by VT ¹H NMR. This situation is similar for the C1 conformer.

In contrast, the near symmetric potential associated with 8-PnMGO and 8-PinMGO (Fig. 7) is in accord with the negligible change in chemical shift with temperature for these compounds, since the increase in *T* will not change significantly the conformers' relative population. As can be seen in Fig. 9 (bottom), conformer B₁ places the imine proton in a deshielding region of the phenyl ring, while conformer B₃ places it in a shielding region of the aromatic ring current. In conformer B₂ the phenyl and methyl groups are sufficiently far away and no significant shielding/deshielding effects are expected. This implies that the observed δ (ppm) has a shielding contribution from the B₃ conformer, and a deshielding contribution from the B₁ conformer. Given the symmetry of the derived torsional potential, conformers B₁ and B₃ are nearly isoenergetic and, relative to one another, evenly populated at all *T*, contributing with similar weights for the overall shielding effect relative to the phenyl group. These two opposite effects shall nearly cancel each other resulting in an observed chemical shift very similar to that of a simple aldoxime, in nice agreement with the experimental results.

It is also worth noting the nice agreement observed between the theoretical and experimental NOE-NMR results. For 8-PMGO, the only significant NOE effects are those consistent with the A₁ and/or A₃ geometries, in agreement with the higher A₁ population found in the computational calculations. No NOE effect characteristic of the A₂ geometry was observed. For 8-PnMGO and 8-PinMGO, considerable NOE signals were observed for short contacts that are expected to occur in all the B₁, B₂, and B₃ conformations (see Supplementary data for more details), in agreement with the more symmetrical torsional potential calculated for these compounds (Fig. 7).

In Fig. 10 is presented the X-ray crystal structure of 8-PnMGO (4b).¹⁵ As can be seen, the molecular structure corresponds approximately to the optimized B₂ minimum geometry obtained in the gas phase computational calculations.

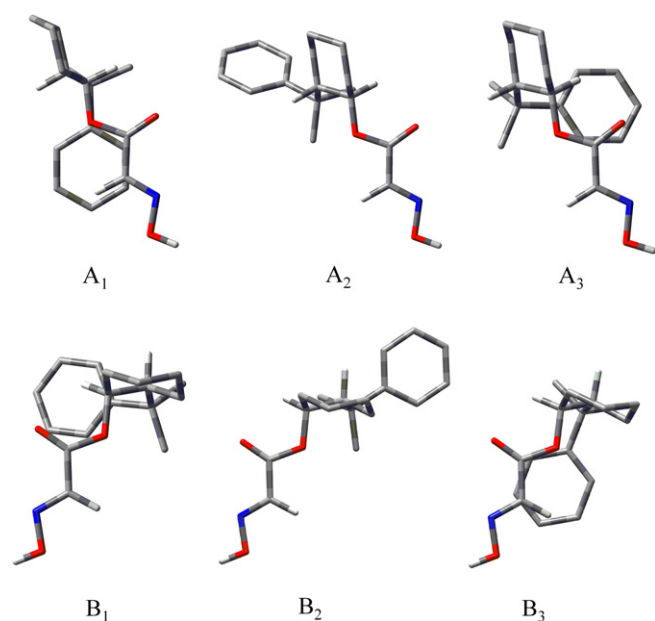


Fig. 9. Optimized geometries at the SCS-MP2/cc-pVDZ level for the minima of the C2 conformer in 8-PMGO (top) and for the minima of 8-PnMGO (bottom). Some hydrogens are omitted for clarity. The pictures emphasize the relative orientation between the imine and phenyl groups.

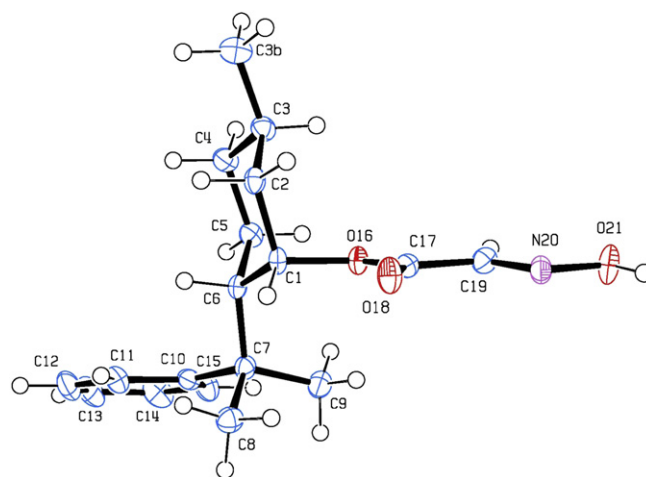


Fig. 10. A view of (+)-8-phenylneomenthyl glyoxylate oxime (4b)¹⁵ showing the atom-labeling scheme. Displacement ellipsoids are drawn at the 50% probability level.

The carbonyl C=O and imine C=N moieties are in the *s*-cis type conformation, whereas the hydroxyl group has *E* configuration. In addition to the O–H···O relatively strong intermolecular interactions, the molecules of 8-PnMGO are linked by intermolecular

$\pi \cdots \pi$ interactions between the phenyl ring and the glyoxylate oxime π system, leading to the formation of [001] chains, as depicted in Fig. 11. The existence of the intermolecular $\pi \cdots \pi$ interaction in 8-PnMGO is a strong proof that these two π systems can indeed interact favorably, thus supporting the existence of its intramolecular counterpart in 8-PMGO and 8-PnMGO/8-PinMGO. 8-PinMGO is structurally very similar to 8-PnMGO, the only difference being the equatorial position of the corresponding C3B methyl group. In 8-PinMGO, the mentioned methyl group will lie partially over the glyoxylate oxime π system and possibly preclude the formation of the intermolecular $\pi \cdots \pi$ interaction with the phenyl ring of a neighboring molecule. These observations can be related with the lower tendency to crystallize observed for 8-PinMGO.

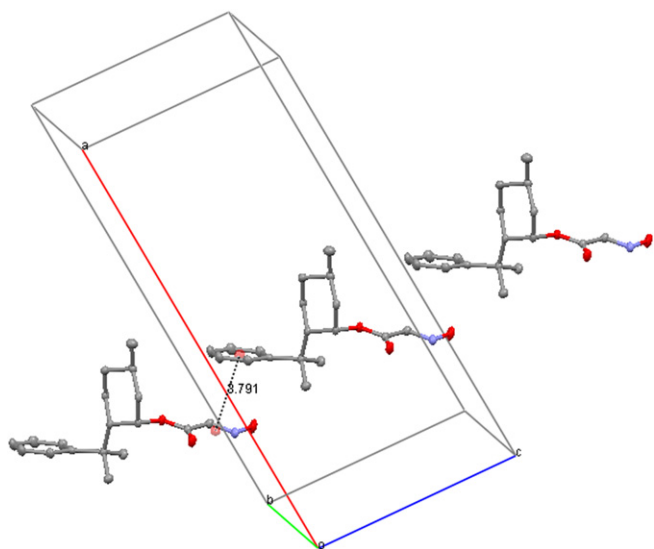
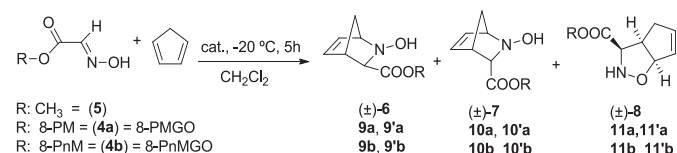


Fig. 11. Part of the crystal structure of 8-PnMGO. Dashed line shows the $\pi \cdots \pi$ interaction between the phenyl ring and the glyoxylate oxime π system (the distance between centroids is 3.791 Å), creating a chain along the [001] direction. H atoms are omitted for clarity.

2.3. Cycloaddition reactions

The cycloaddition reactions are among the most important tools for synthesis in organic chemistry, being crucial for the preparation of natural products and biologically active substances. *N*-Functionalized isoxazolidines have been prepared from 1,3-dipolar cycloadditions between nitrones and alkenes,^{16–18} and their derivatives may possess antifungal,¹⁹ antibacterial,²⁰ and antiviral activities.²¹ The preparation of non-functionalized isoxazolidines was previously reported.^{8,22} A detailed mechanistic study on the cycloaddition reaction between CPD and methyl glyoxylate oxime (**5**) under acid catalysis, affording a mixture of the aza-Diels–Alder reaction products [*exo* and *endo* isomers of (\pm)-2-hydroxy-2-azabicyclo[2.2.1]hept-5-ene-3-carboxylate, **6** and **7**, respectively] and the 1,3-cycloaddition adduct [methyl (1*RS*,4*RS*,5*RS*)-(2-oxa-3-azabicyclo[3.3.0]oct-7-ene)-4-carboxylate, **8**], was also reported (Scheme 2) by our research group.^{8b}



Scheme 2. Cycloaddition reaction between methyl glyoxylate oxime (**5**) and CPD, under acid catalysis. 8-PM-(–)-8-phenylmenthyl; 8-PnM-(+)-8-phenylneomenthyl.

In this work, the cycloaddition reactions between 8-PMGO/8-PnMGO and CPD were performed according to our method,⁸ as represented in Scheme 2, using BF₃ or H⁺ (trifluoroacetic acid, TFA) as catalysts at –20 °C. Table 1 summarizes the results in terms of total yield, selectivity for the 1,3- over the 1,4-cycloaddition (aza-Diels–Alder) and the ratio of the two diastereoisomers of **11** (**a** or **b**) obtained from the cycloaddition reaction. The cycloaddition reaction with 8-PinMGO (**4c**) was not performed because 8-phenylisoneomenthol (**1c**) is a minor product in the synthesis of 8-phenylmenthol isomers, and the application and evaluation of **1c** as chiral auxiliary was already described for aza-Diels–Alder reactions in terms of its enantioselectivity.^{3g}

Table 1

Total yield (η), regioselectivity, and 1,3-cycloaddition diastereoselectivity obtained for the reactions between **4a,4b** and CPD

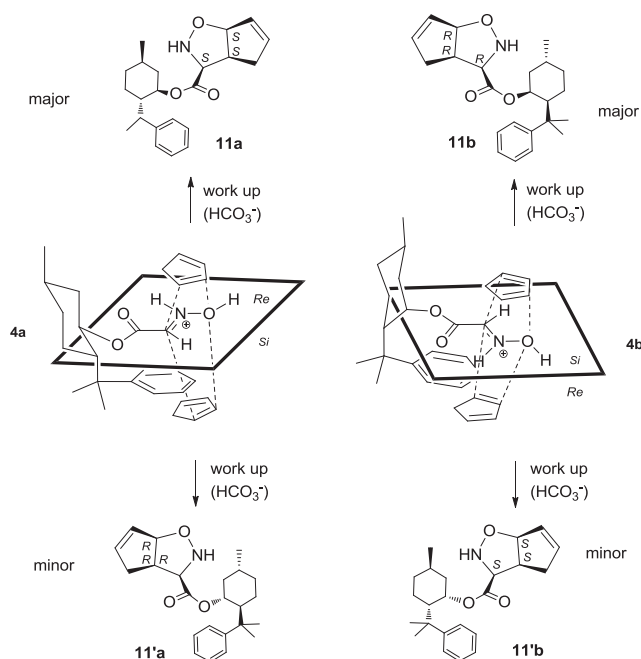
Entry	Oxime	Cat.	$\eta_{\text{total}}/\%$	Selectivity (%) 1,3 vs 1,4 cycloaddition ^a	Selectivity (%) 11/11' ^a
1	8-PMGO	—	— ^b	—	—
2		TFA	40	60	91/09
3		BF ₃	32	80	80/20
4	8-PnMGO	TFA	38	60	78/22
5		BF ₃	36	75	73/27

^a Values determined from ¹H NMR analyses of the mixture of the obtained adducts.

^b Traces of **11a** were detected by ¹H NMR analysis.

As in the previously reported cycloaddition between **5** and CPD,⁸ the total yield of the reaction was moderate, the starting material being partially recovered. In the same way, the 1,3-cycloaddition was preferred over the 1,4-cycloaddition, in particular when BF₃ was used as catalyst. Only the asymmetric induction of the 1,3-cycloaddition reaction was evaluated, as the aza-Diels–Alder adducts **9** and **10** (**a** or **b**) were clearly the minor products over **11** (see Supplementary data). Hence, for each performed reaction, the diastereoisomeric ratios **11a/11'a** or **11b/11'b** were quantified by ¹H NMR analysis of the reaction mixture.

Considering the structures of 8-PMGO and 8-PnMGO in CH₂Cl₂ solution in the presence of a catalyst as TFA (H⁺), one can rationalize the outcome of the cycloaddition reaction according to Scheme 3. The presence of a catalyst as BF₃ leads to comparable results, the **11/11'** selectivity being slightly lower. This result agrees well with the previously reported mechanism, which states that BF₃ coordinates to the oxygen atom of the hydroxyl group promoting a prototropic displacement of the hydroxyl hydrogen to the nitrogen atom, forming a BF₃–nitron complex.^{8b} So, in practical terms, the use of either H⁺ or BF₃ results in the *N*-protonation of the oxime, thus stabilizing the *s-cis* conformation by about 10 kJ mol^{–1} due to the formation of an intramolecular hydrogen bond with the carbonyl oxygen.^{8b} In the case of 8-PMGO, CPD will effectively approach by the sterically unobstructed *Re* face of the nitrogen trigonal atom, affording (–)-8-phenylmenthyl (1*S*,4*S*,5*S*)-(2-oxa-3-azabicyclo[3.3.0]oct-7-ene)-4-carboxylate (**11a**) as major product. Similarly, CPD efficiently approaches by the sterically unhindered *Si* face of 8-PnMGO, giving (+)-8-phenylneomenthyl (1*R*,4*R*,5*R*)-(2-oxa-3-azabicyclo[3.3.0]oct-7-ene)-4-carboxylate (**11b**) as the major diastereoisomer. Despite only the products of the 1,3-cycloaddition were considered and properly quantified and characterized, the stereochemistry of the minor adducts that result from 1,4-cycloaddition may be analogously rationalized. The stereochemistry of the identified aza-Diels–Alder adducts, as well as the comparative quantification when each catalyst was employed, are presented in Supplementary data.



Scheme 3. Representation of the CPD approach to the oximes **4a** (8-PMGO) and **4b** (8-PnMGO) to afford the respective 1,3-cycloadducts. From the usage of BF_3 as catalyst would result a similar figure, the BF_3 substituting the hydroxyl's group hydrogen.

It was verified that some of the obtained diastereoisomers possess identical R_f in various eluents, which makes their separation a rather difficult task. Therefore, some of the compounds were characterized as a mixture of two pairs of diastereoisomers. By this reason, along with the fact of being minor adducts, their precise quantification was not possible.

In what concerns the possible *E/Z* isomerization relative to the oxime moiety, it seems realistic to assume that *E* conformation is preferred, in particular in solution and crystal phases; in fact, this preference is quite standard for glyoxylate derived oximes.^{8,23} Nevertheless, the hypothetical *E/Z* isomerization occurring with cycloaddition reactions would be irrelevant, since the nitrogen atom in the final adduct exists as a tertiary amine capable of undergoing inversion of the lone pair of electrons to achieve the most stable conformation.

Based on the computational study presented in Section 2.2, the **11/11'** stereoselectivity (Table 1) can in principle be reproduced on quantitative terms. For that, the relative populations of all relevant stable conformations of 8-PMGO and 8-PnMGO/8-PinMGO need to be known. However, since the reaction takes place after protonation of the oxime's nitrogen (either directly by TFA or indirectly by BF_3) the resulting protonated species must be considered. Since a full conformational study is still a hard task to perform adequately on these relative large molecular systems, the following approximations were employed: (1) the conformational distributions associated to the potential energy profiles for internal rotation about the C(R)–C–C–Ph dihedral for the C1 conformer of 8-PnMGO (Fig. 7), and the C1 and C2 conformers of 8-PMGO (Fig. 8) were assumed to be unchanged after protonation; (2) the *s-cis/s-trans* equilibrium presented in Fig. 4 for the protonated species were evaluated based on the calculations performed for $R'=\text{CH}_3$ (with and without BF_3 coordinated to the hydroxyl's oxygen). These assumptions are valid if after protonation the reaction takes place relatively fast, allowing only *s-cis/s-trans* interconversion to occur and preventing the slower interconversions connected by the C(R)–C–C–Ph dihedral angle. Moreover, one must assume that the *s-cis/s-trans* equilibria are independent of R' (Fig. 4). Considering

these approximations, the statistical population of each conformer, p_i , was calculated using the Boltzmann equation:

$$p_i = \frac{\exp(-E_i/RT)}{\sum \{\exp(-E_i/RT)\}} \quad (1)$$

where the temperature, T , used was equal to the experimental conditions ($T=253$ K), R is the ideal gas constant, and E_i is the relative energy of each conformer, i , calculated by superimposing $\Delta E(s\text{-cis}/s\text{-trans})$ for $R'=\text{CH}_3$ to all minima presented in Figs. 7 and 8. The calculated statistical distributions for 8-PMGO and 8-PnMGO using TFA as catalyst are presented in Tables 2 and 3, respectively. The results using no catalyst and using BF_3 as catalyst are presented in the Supplementary data.

Table 2

Calculated statistical distribution of all relevant conformers of 8-PMGO, at $T=253$ K, considering TFA as the catalyst

Conformer	$E_{\text{rel}}/\text{kJ mol}^{-1}$	$p_i/\%$	11/11' Selectivity efficiency	
C1	A ₁ cis	7.5	2.5	0/100
	A ₁ trans	17.8	0.0	100/0
	A ₂ cis	14.1	0.1	50/50
	A ₂ trans	24.4	0.0	50/50
	A ₃ cis	17.1	0.0	33/67
	A ₃ trans	27.4	0.0	67/33
C2	A ₁ cis	0.0	88.6	100/0
	A ₁ trans	10.3	0.7	0/100
	A ₂ cis	6.5	4.0	50/50
	A ₂ trans	16.8	0.0	50/50
	A ₃ cis	6.5	4.0	67/33
	A ₃ trans	16.8	0.0	33/67

Table 3

Calculated statistical distribution of all relevant conformers of 8-PnMGO, at $T=253$ K, considering TFA as the catalyst

Conformer	$E_{\text{rel}}/\text{kJ mol}^{-1}$	$p_i/\%$	11/11' Selectivity efficiency	
C1	B ₁ cis	0.0	47.4	67/33
	B ₁ trans	10.3	0.4	33/67
	B ₂ cis	2.5	14.4	50/50
	B ₂ trans	12.8	0.1	50/50
	B ₃ cis	0.5	37.4	100/0
	B ₃ trans	10.8	0.3	0/100

As can be inferred from the molecular geometries presented in Fig. 9, each conformer is more or less effective in inducing stereoselectivity. For instance, in A₁ the *Si* face of the oxime is almost completely blocked by the phenyl ring, virtually excluding the possibility of a CPD attack from that side. In A₂ neither face is blocked, hence no stereoselectivity is expected from this conformer. A *Re/Si* selectivity for the CPD approach (and consequently the formation of **11/11'**) of 100/0 and 50/50 was assumed to each case, respectively. However, for conformers A₃ and B₁ there is an intermediate selectivity, one face being only partially blocked by the phenyl ring. For these cases, the CPD approach for the attack from the unobstructed face was assumed to be twice as probable as from the more obstructed one, which gives a selectivity of 67/33. Although this is only a rough approximation, we believe that it is a reasonable value: in the A₃ and B₁ conformers (Fig. 9) nearly a half of one face of the glyoxylate oxime π system is blocked by the phenyl ring. The sum-product of p_i and **11/11'** selectivity efficiency then yields the expected total stereoselectivity of 8-PMGO and 8-PnMGO. Table 4 presents the calculated selectivity for **11** associated to these compounds when TFA and BF_3 were used as catalysts. The calculated **11** selectivity that would be expected if no catalyst was used is also presented for comparison.

Table 4

Experimental and calculated **11** selectivity associated to 8-PMGO and 8-PnMGO using no catalyst, and TFA and BF₃ as catalysts

Oxime	Catalyst	11 Selectivity	
		Experimental	Calculated
8-PMGO	—	—	37
	TFA	91	93
	BF ₃	80	76
8-PnMGO	—	—	42
	TFA	78	77
	BF ₃	73	66

Table 3 shows that this simple conformational analysis does a good job on quantitatively predicting the stereoselectivity in cycloaddition reactions using 8-PMGO and 8-PnMGO/8-PinMGO as chiral auxiliaries. The calculated **11/11'** selectivities must be treated with care since some important approximations, which may not exactly hold, were considered in our methodology. However, this study points out that stereoselectivity in these systems is crucially linked to conformational distribution, which in turn is dictated by intramolecular interactions. The use of catalysts, such as TFA or BF₃ can have an important influence on conformational distribution. For instance, without protonation of the oxime's nitrogen, the *s*-cis conformer would not be favored to any significant extent, and thus a lower stereoselectivity would be expected. The lower **11** selectivity using BF₃ can be explained by the fact that $\Delta E(s\text{-cis} \rightarrow s\text{-trans})$ is of 10.3 kJ mol⁻¹ for TFA and of only 3.0 kJ mol⁻¹ for BF₃. For 8-PinMGO, a selectivity efficiency similar to 8-PnMGO is expected, but with the opposite stereo configuration.

3. Conclusions

The establishment of the structures of the titled compounds in solution is of great assistance for the prediction and interpretation of the outcome of asymmetrical synthesis in which the stereoisomers of 8-phenylmenthol are employed as chiral auxiliaries. From this study we conclude that 8-PMGO and 8-PinMGO block the *Si* face (regarding the trigonal nitrogen atom) of the glyoxylic moiety and 8-PnMGO hinders the *Re* face; additionally, *Si* face is expected to be more efficiently blocked if (–)-8-phenylmenthol is preferred over (–)-8-phenylisoneomenthol.

The prediction of the cycloadduct's stereochemistry in asymmetrical aza-Diels–Alder reactions, based on the combination of these findings with the knowledge of the reaction mechanism, is in complete agreement with experimental results involving glyoxylate imines derived from stereoisomers of 8-phenylmenthol.^{3fg} In this particular work we were able to qualitatively and quantitatively predict the stereochemistry of both 1,3- and 1,4-cycloaddition of CPD with glyoxylate oximes derived from stereoisomers of 8-phenylmenthol with excellent accuracy.

4. Experimental

4.1. General

All reactions were carried out under anhydrous conditions. Solvents were dried according to standard procedures and distilled prior to use. All reagents were commercially available and used without further purification, unless otherwise stated. Flash column chromatography was performed on silica gel (60Å, 230,240 mesh) and analytical thin-layer chromatography (TLC) on pre-coated silica gel 60 F₂₅₄ plates using iodine vapor and/or UV light (254 nm) for visualization. Melting points were determined on an electrothermal melting point apparatus and are uncorrected. Optical rotations

were measured on a conventional thermostated polarimeter using a sodium lamp. Elementary analyses were obtained on a micro-analyser apparatus.

4.2. NMR spectroscopy

NMR analyses were performed in a Bruker Avance III 400, equipped with a 5 mm broad band observe (bbo) probe, using TMS as internal standard for ¹H and ¹³C, and NH₃ for ¹⁵N nucleus (¹⁵N chemical shifts were recorded as HMBC). Low temperatures were achieved by cooling the sample in the probe by means of flowing vapor of liquid nitrogen. Temperature calibrations were performed with a 4% MeOH in MeOD-*d*₄ solution. The overall uncertainty associated with the temperature measurements is estimated as ±1 K. NMR analysis of **2b** was performed in a Bruker AMX 300.

4.3. Computational details

All theoretical calculations were performed using the Gaussian 03 software package.²⁴ The full and partial geometry optimizations for 1-(2-cyclohexylpropan-2-yl)benzene, 8-PMGO, and 8-PnMGO were performed using the Moller–Plesset perturbation theory with a second order perturbation (MP2) and the correlation consistent basis set cc-pVDZ.

4.4. X-ray crystallography

Crystals of 8-PnMGO were obtained by slow evaporation of a dichloromethane/methanol solution. Data collection, cell refinement, and data reduction were made with the software package of a Bruker AXS APEX II-CCD area detector diffractometer. Absorption correction was performed with SADABS.²⁵ The structure was solved using the software SIR97²⁶ and refined with SHELXL97.²⁷ Molecular graphics were produced by ORTEP,²⁸ MERCURY,²⁹ and PLATON.³⁰ The complete set of structural parameters in CIF format is available as an Electronic Supplementary Publication from the Cambridge Crystallographic Data Centre (CCDC 787450).¹⁵ Information about crystal data, data acquisition conditions, and refinement parameters are presented in Supplementary data. All H atoms were found in a differential Fourier map and placed geometrically idealized and constrained to ride on their parent atoms [*C*–H=0.95–1.00 Å and *U*_{iso}(H)=1.2 and 1.5 *U*_{eq}(C)].

4.5. Mass spectrometry

ESI-MS analyses were performed on a liquid 35 chromatography Finnigan Surveyor equipment, coupled to a mass detector Finnigan LQC DECA XP MX with an API and an ESI interface. HRMS were performed by ESI-TOF analyses on a Bruker Microtof equipment coupled to an HPLC Agilent 1100.

4.6. Synthesis

4.6.1. General procedure for the synthesis of 2a–c. To a solution of pure **1a** (0.76 g, 3.2 mmol) in dry dichloromethane (10 ml) under argon atmosphere, a catalytic amount of DMAP (ca. 5%) and triethylamine (0.92 ml, 6.6 mmol) were added. The solution was placed into an ice bath and a solution of acryloyl chloride (0.54 ml, 6.6 mmol) in dry dichloromethane (4 ml) was slowly added. The mixture was left to react during 3 h in an ice bath. After addition of water (20 ml), the phases were separated and the aqueous layer was extracted with dichloromethane (3×20 ml). The organic layers were dried over anhydrous Na₂SO₄, filtered and the solvent removed at reduced pressure. After flash chromatography (SiO₂), a yellow oil **2a** was obtained (η =89%). Similar procedure was

adopted for the synthesis of **2b** ($\eta=87\%$) and **2c** ($\eta=85\%$) from the corresponding alcohols.

4.6.1.1. (1R,2S,5R)-5-Methyl-2-(2-phenylprop-2-yl)cyclohexyl acrylate (2a). ^1H NMR (400 MHz, CDCl_3): $\delta=7.21\text{--}7.29$ (m, 4H_{Ph}), 7.0–7.13 (m, 1H, H_{para}), 5.96–6.05 (m, 1H, CH=CH_aH_b), 5.54–5.62 (m, 2H, CH=CH_aH_b and CH=CH₂), 4.86 (dt, $J=10.7$, 4.4 Hz, 1H, H_{18-PM}), 1.30 and 1.22 (2s, 6H, 8'-(CH₃)₂), 0.86 (d, $J=6.5$ Hz, 3H, 5'-CH₃), 2.00–2.09 (m, 1H), 1.88–1.95 (m, 1H), 1.60–1.71 (m, 2H), 1.42–1.54 (m, 1H), 0.90–1.16 (m, 3H). ^{13}C NMR (100 MHz, CDCl_3): $\delta=165.4$ (COO), 151.5 (C_{ipso}), 129.9 (C3), 128.9 (C2), 128.0 (C_{Ph}), 125.4 (C_{Ph}), 125.0 (C_{Ph}), 74.5 (CH), 50.5 (CH), 41.6 (CH₂), 39.7 (C8'), 34.6 (CH₂), 31.3 (CH), 27.5 (8'-CH₃), 26.6 (CH₂), 25.3 (8'-CH₃), 21.8 (5'-CH₃); ESI-MS: calculated for [C₁₉H₂₆O₂+H]⁺ (M+H⁺) 287.19, found 287.52; $[\alpha]_D^{25} -9.5$ (c 1, CHCl₃).

4.6.1.2. (1S,2S,5R)-5-Methyl-2-(2-phenylprop-2-yl)cyclohexyl acrylate (2b). ^1H NMR (300 MHz, CDCl_3): $\delta=7.16\text{--}7.30$ (m, 5H_{Ph}), 6.35 (dd, $J=17.3$, 1.5 Hz, 1H, CH=CH_aH_b), 6.08 (dd, $J=17.3$, 10.4 Hz, 1H, CH=CH₂), 5.80 (dd, $J=10.4$, 1.5 Hz, 1H, CH=CH_aH_b), 5.04 (s, 1H, H_{18-PinM}), 1.53–1.97 (m, 6H, CH₂), 1.35 (s, 6H, 8'-(CH₃)₂), 0.84 (d, $J=6.3$ Hz, 3H, 5'-CH₃). ^{13}C NMR (75 MHz, CDCl_3): $\delta=165.6$ (COO), 149.8 (C_{ipso}), 130.5 (C3), 129.8 (C2), 128.4 (C_{Ph}), 126.4 (C_{Ph}), 126.0 (C_{Ph}), 71.9 (CH), 51.7 (CH), 40.3 (C8), 35.8 (CH₂), 30.2 (CH₂), 27.3 (8'-CH₃), 27.1 (8'-CH₃), 26.5 (CH), 22.9 (CH₂), 22.5 (5'-CH₃); ESI-MS: calculated for [C₁₉H₂₆O₂+H]⁺ (M+H⁺) 287.19, found 287.56; $[\alpha]_D^{25} +53.1$ (c 1, CHCl₃).

4.6.1.3. (1R,2R,5R)-5-Methyl-2-(2-phenylprop-2-yl)cyclohexyl acrylate (2c). ^1H NMR (400 MHz, CDCl_3): $\delta=7.18\text{--}7.44$ (m, 5H_{Ph}), 6.35 (dd, $J=17.4$, 1.4 Hz, 1H, CH=CH_aH_b), 6.09 (dd, $J=17.4$, 10.4 Hz, 1H, CH=CH₂), 5.83 (dd, $J=10.4$, 1.4 Hz, 1H, CH=CH_aH_b), 5.00 (s, 1H, H_{18-PinM}), 1.45–1.98 (m, 6H, CH₂), 1.35 and 1.36 (2s, 6H, 8'-(CH₃)₂), 1.01 (d, $J=7.4$ Hz, 3H, 5'-CH₃). ^{13}C NMR (100 MHz, CDCl_3): $\delta=166.1$ (COO), 150.2 (C_{ipso}), 131.0 (C3), 130.4 (C2), 128.9 (C_{Ph}), 126.9 (C_{Ph}), 126.4 (C_{Ph}), 72.8 (CH), 52.4 (CH), 41.1 (C8), 37.1 (CH₂), 33.1 (CH₂), 27.6 (8'-CH₃), 26.7 (CH), 27.4 (8'-CH₃), 21.3 (5'-CH₃), 18.3 (CH₂); ESI-MS: calculated for [C₁₉H₂₆O₂+H]⁺ (M+H⁺) 287.19, found 287.53.

4.6.2. General procedure for the synthesis of 3a–c.^{2,3d} To a stirring solution of **2a–c** (0.50 g, 1.75 mmol) in 3/1 dioxane/water (20 ml), a 0.01 M solution of OsO₄ in dioxane/water 3/1 (1.1 ml) was added. After 5 min, NaIO₄ (0.75 g, 3.50 mmol) was added in small portions and the mixture was left to react overnight. After addition of water (30 ml), the mixture was extracted with ethyl acetate (3×30 ml). The organic layers were dried over anhydrous Na₂SO₄, filtered and the solvent removed at reduced pressure to afford the corresponding glyoxylates **3a–c** (yields: **3a**–99%; **3b**–91%; **3c**–90%). No purification was needed, the product being used directly in the next reaction.

4.6.3. Procedure for the synthesis of oximes

4.6.3.1. 8-PMGO (4a). To 2.30 g (33.1 mmol) of NH₂OH·HCl in anhydrous dichloromethane (30 ml), a catalytic amount of DMAP (ca. 5%), anhydrous triethylamine (4.65 ml, 33.4 mmol) and 8-phenylmenthyl glyoxylate **3a** (0.95 g, 32.0 mmol) were added. The mixture was left to react overnight under argon atmosphere at room temperature. After addition of water (20 ml) and subsequent phase separation, the aqueous layer was extracted with dichloromethane (3×20 ml). The organic extracts were dried over anhydrous Na₂SO₄ and the solvent evaporated under low pressure. When necessary, purification was performed by flash chromatography (SiO₂, Hex/AcOEt). Similar procedures were adopted for the synthesis of 8-PnMGO and 8-PinMGO. Virtually unitary yields were obtained.

4.6.3.2. 8-PMGO (4a). ^1H NMR (400 MHz, CDCl_3): $\delta=9.91$ (br s, OH), 7.11–7.29 (m, 4H_{Ph}), 7.10–7.15 (m, 1H, H_{para}), 6.79 (s, 1H, H_{imine}), 4.98 (dt, $J=10.7$, 4.5 Hz, 1H, H_{18-PM}), 2.04–2.13 (m, 1H), 1.86–1.94 (m, 1H), 1.76–1.83 (m, 1H), 1.63–1.71 (m, 1H), 1.41–1.55 (m, 1H), 1.23 and 1.31 (2s, 6H, 8'-(CH₃)₂), 0.90–1.20 (m, 4H), 0.88 (d, $J=6.5$ Hz, 5'-CH₃); ^{13}C NMR (100 MHz, CDCl_3): $\delta=161.2$ (COO), 151.1 (C_{ipso}), 141.7 (C=N), 128.0 (C_{Ph}), 125.3 (C_{Ph}), 125.1 (C_{para}), 75.5 (C_{18-PM}), 50.4, 41.4, 39.5, 34.3, 31.2, 28.5, 26.3, 24.0, 21.7; ^{15}N NMR (40 MHz, CDCl_3): $\delta=396$; ESI-TOF: calculated for [C₁₈H₂₆NO₃+Na]⁺ (M+Na⁺) 326.17, found 326.1724; $[\alpha]_D^{22} -1.5$ (c 1, CHCl₃);

4.6.3.3. 8-PnMGO (4b). ^1H NMR (400 MHz, CDCl_3): $\delta=9.30$ (br s, OH), 7.45 (s, 1H, H_{imine}), 7.25–7.30 (m, 4H_{Ph}), 7.15–7.20 (m, 1H, H_{para}), 5.07 (s, H_{18-PinM}), 1.89–1.93 (m, 1H), 1.72–1.79 (m, 1H), 1.55–1.70 (m, 5H), 1.33 and 1.34 (2s, 6H, 8'-(CH₃)₂), 1.00–1.08 (m, 1H), 0.89–0.92 (m, 1H), 0.81 (d, $J=6.6$ Hz, 3H, 5'-CH₃); ^{13}C NMR (100 MHz, CDCl_3): $\delta=162.5$ (COO), 149.9 (C_{ipso}), 142.8 (C=N), 129.0 (C_{Ph}), 126.9 (C_{Ph}), 126.7 (C_{para}), 74.2 (C_{18-PinM}), 52.1, 40.9, 40.6 (CH₂), 36.1 (CH₂), 28.0, 27.6, 26.9, 23.2 (CH₂), 22.0; ^{15}N NMR (40 MHz, CDCl_3): $\delta=396$; ESI-MS: calculated for [C₁₈H₂₆NO₃+H]⁺ (M+H⁺) 304.26, calculated for [C₁₈H₂₆NO₃+Na]⁺ (M+Na⁺) 326.17, found 304.28 and 326.25; $[\alpha]_D^{24} +47.0$ (c 1, CHCl₃); mp=119–121 °C.

4.6.3.4. 8-PinMGO (4c). ^1H NMR (400 MHz, CDCl_3): $\delta=10.10$ (br s, OH), 7.50 (s, 1H, H_{imine}), 7.30–7.33 (m, 4H_{Ph}), 7.18–7.25 (m, 1H, H_{para}), 5.05 (s, H_{18-PinM}), 1.80–2.00 (m, 4H), 1.45–1.70 (m, 5H), 1.38 and 1.39 (2s, 6H, 8'-(CH₃)₂), 1.02 (d, $J=7.4$ Hz, 3H, 5'-CH₃); ^{13}C NMR (100 MHz, CDCl_3): $\delta=162.3$ (COO), 149.8 (C_{ipso}), 143.1 (C=N), 129.0 (C_{Ph}), 126.9 (C_{Ph}), 125.6 (C_{para}), 74.7 (C_{18-PinM}), 52.3; 41.1, 37.1 (CH₂), 33.0 (CH₂), 28.2, 27.0, 26.5, 21.2, 18.24 (CH₂); ^{15}N NMR (40 MHz, CDCl_3): $\delta=398$; ESI-TOF: calculated for [C₁₈H₂₆NO₃+Na]⁺ (M+Na⁺) 326.17, found 326.1724; $[\alpha]_D^{24} -50.2$ (c 1, CHCl₃).

4.6.4. General procedure for the acid-mediated cycloaddition reaction of oximes (4a and 4b) with CPD. To a stirred solution of oxime **4** (0.50 g, 1.7 mmol) in dry CH₂Cl₂ (15 ml) under argon atmosphere, at temperature –20 °C, the catalyst (1 equiv, according to Table 3) and CPD (0.14 ml, 1.7 mmol) were added. After the mixture was left to react during 2.5 h, additional CPD (0.14 ml, 1.7 mmol) was added and the reaction was left to react during further 2.5 h. The reaction mixture was neutralized with aqueous saturated solution of NaHCO₃ (7 ml) and was allowed to heat to the room temperature under stirring overnight. The two phases were separated and the aqueous phase was extracted with CH₂Cl₂ (3×15 ml). The organic extracts were rinsed with brine, dried, and evaporated. The obtained residue was washed and triturated under methanol (15 ml); after filtration through a Büchner funnel with Celite plus silica under reduced pressure, all the precipitate was removed to give a clear solution that was evaporated again. The oily mixture was submitted to chromatographic columns (SiO₂, Hex/AcOEt, 1/1), the fractions corresponding to two distinct compositions being separated and being subject of a new chromatographic column each (first mixture, SiO₂, Hex/AcOEt, 1/2; second mixture, SiO₂, Hex/AcOEt, 1/3). The process was repeated when necessary until they succeed to obtain good NMR spectra. None of the compounds was fully isolated, the yields being determined by NMR and present in Table 3.

4.6.4.1. Compound 9a. ^1H NMR (400 MHz, CDCl_3): $\delta=7.25\text{--}7.36$ (m, 5H_{Ph}), 7.10–7.19 (m, 1H_{Ph}), 6.43–6.48 (m, 1H, H5), 6.24 (dd, $J=5.6$, 2.0 Hz, 1H, H6), 4.94 (m, H_{18PM}), 4.21 (s, 1H, H1), 2.68 (s, 1H, H4), 2.30 (d, $J=2.1$ Hz, 1H, H3), 1.35–2.15 (m, 5H_{8-PM+H7_{syn}+H7_{anti}}), 1.59 (d, $J=9.2$ Hz, 1H_{8-PM}), 1.21 and 1.33 (2s, 6H, 8-(CH₃)_{2-8PM}), 0.90–1.20 (m, H_{28-PM}), 0.88 (d, $J=6.5$ Hz, H3, 5-CH_{3-8PM}); ^{13}C NMR (100 MHz, CDCl_3): $\delta=171.6$ (COO), 151.7 (8-C_{ipso}), 137.9 (C5), 133.1 (C6), 128.0 (2× C_{Ph}), 125.4 (2× C_{Ph}),

125.0 (C_{para}), 75.0 (C_{18PM}), 70.5 (C3), 69.0 (C1), 50.4 (C_{28PM}), 47.2 (C4), 45.0 (C7), 41.6 (CH_2), 39.6 (C_{8-PM}), 34.6 (CH_2), 31.2 (C_{58PM}), 26.5 (CH_2), 24.7 and 28.1 ($2 \times 8-CH_3-8PM$), 21.8 ($5-CH_3-8PM$); ^{15}N NMR (40 MHz, $CDCl_3$): $\delta=148$.

4.6.4.2. Compound 11a. 1H NMR (400 MHz, $CDCl_3$): $\delta=7.27-7.37$ (m, 5 H_{Ph}), 7.14–7.21 (m, 1 H_{Ph}), 6.00–6.05 (m, 1H, H8), 5.58 (ddd, $J=5.6, 4.3, 2.1$ Hz, 1H, H7), 5.29 (d, $J=6.8$ Hz, 1H, H1), 5.05–5.45 (br s, 1H, NH), 4.89 (dt, $J=10.8, 4.4$ Hz, 1H, H_{18PM}), 3.09 (d, $J=8.1$ Hz, 1H, H4), 2.95–3.30 (m, 1H, H5), 2.31–2.40 (m, 1H, H_{6syn}), 2.05–2.13 (m, 1 H_{8-PM}), 2.01 (dq, $J=18.2, 2.3$ Hz, 1H, H_{6anti}), 1.86–1.94 (m, 1 H_{8-PM}), 1.81 (dq, $J=13.4, 3.4$ Hz, 1 H_{8-PM}), 1.67–1.74 (m, 1 H_{8-PM}), 1.43–1.55 (m, 2 H_{8-PM}), 1.32 and 1.23 (2s, 6H, 8-(CH_3) $_2$ -8PM), 1.13–1.19 (m, 1 H_{8-PM}), 0.97–1.03 (m, 1 H_{8-PM}), 0.91 (d, $J=6.5$ Hz, 3H, 5- CH_3 -8PM); ^{13}C NMR (100 MHz, $CDCl_3$): $\delta=169.7$ (COO), 152.4 (8- C_{ipso}), 138.4 (C8), 128.9 ($2 \times C_{Ph}$) and 129.0 ($2 \times C_{Ph}$), 126.2 (C7), 126.1 (C_{para}), 92.7 (C1), 76.2 (C_{18PM}), 66.7 (C4), 51.2 (C_{28PM}), 46.3 (C5), 42.3 (CH_2), 40.4 (C_{88PM}), 35.4 (C6), 35.4 (CH_2), 32.2, 29.6, 27.3 (CH_2), 24.9, 22.7; ^{15}N NMR (40 MHz, $CDCl_3$): $\delta=142$; ESI-TOF: calculated for $[C_{23}H_{31}NO_3+H]^+$ ($M+H^+$) 370.23, found 370.2377, $[\alpha]_D^{25} -19.2$ (c 0.32, $CHCl_3$).

4.6.4.3. Compound 11a'. 1H NMR (400 MHz, $CDCl_3$): $\delta=7.27-7.37$ (m, 5 H_{Ph}), 7.14–7.21 (m, 1 H_{Ph}), 6.08–6.12 (m, 1H, H8), 5.63 (ddd, $J=5.6, 4.3, 2.1$ Hz, 1H, H7), 5.37 (d, $J=6.6$ Hz, 1H, H1), 5.05–5.45 (br s, 1H, NH), 4.86 (dt, $J=10.8, 4.3$ Hz, 1H, H_{18PM}), 3.69 (d, $J=7.7$ Hz, 1H, H4), 3.16–3.23 (m, 1H, H5), 2.40–2.49 (m, 1H, H_{6syn}), 2.24–2.31 (m, 1H, H_{6anti}), 0.93–2.14 (m, 8 H_{8-PM}), 1.37 and 1.26 (2s, 6H, 8-(CH_3) $_2$ -8PM), 0.88 (d, $J=6.5$ Hz, 3H, 5- CH_3 -8PM); ^{13}C NMR (100 MHz, $CDCl_3$): $\delta=169.6$ (COO), 152.0 (8- C_{ipso}), 138.6 (C8), 129.3 ($2 \times C_{Ph}$) and 128.8 ($2 \times C_{Ph}$), 126.7 (C7), 126.3 (C_{para}), 77.9 (C1), 73.2 (C_{18PM}), 69.3 (C4), 50.8 (C_{28PM}), 46.6 (C5), 42.5 (CH_2), 41.0 (C_{88PM}), 39.1 (CH_2), 35.3 (CH_2), 32.3, 29.1, 28.0 (CH_2), 25.5, 22.6; ^{15}N NMR (40 MHz, $CDCl_3$): $\delta=142$.

4.6.4.4. Compound 9b. 1H NMR (400 MHz, $CDCl_3$): $\delta=7.29-7.34$ (m, 5 H_{Ph}), 7.16–7.23 (m, 1 H_{Ph}), 6.64–6.67 (m, 1H, H5), 6.31 (dd, $J=5.6, 2.0$ Hz, 1H, 6-H), 4.95–5.10 (1H, H_{18-PnM}), 4.31 (s, 1H, H1), 3.19 (s, 1H, H4), 2.77 (d, $J=2.1$ Hz, 1H, H3), 1.52–1.96 (m, 5 $H_{8-PnM}+H_{7syn}+H_{7anti}$), 1.45–1.50 (m, 1 H_{8-PnM}), 1.33 and 1.38 (2s, 6H, 8-(CH_3) $_2$ -8PnM), 0.87–1.52 (m, 2 H_{8-PnM}), 0.83–0.86 (3H, 5- CH_3 -8PnM); ^{13}C NMR (100 MHz, $CDCl_3$): $\delta=171.7$ (COO), 149.4 (8- C_{ipso}), 138.1 (C5), 133.2 (C6), 127.8–128.1 ($2 \times C_{Ph}$), 125.5–126.0 ($3 \times C_{Ph}$), 72.1 (C_{18-PnM}), 70.5 (C3), 68.7 (C1), 51.2 (C_{28PnM}), 46.9 (C4), 45.2 (C7), 39.6–40.0 ($C_{8-PnM}+CH_2$), 35.3 (CH_2), 26.0–27.1 ($C_{58-PnM}+2 \times 8-CH_3-8PnM$), 22.4 (CH_2), 22.0 (5- CH_3 -8PnM); ^{15}N NMR (40 MHz, $CDCl_3$): $\delta=150$.

4.6.4.5. Compound 9b'. 1H NMR (400 MHz, $CDCl_3$): $\delta=7.29-7.34$ (m, 5 H_{Ph}), 7.16–7.23 (m, 1 H_{Ph}), 6.61–6.64 (m, 1H, H5), 6.31 (dd, $J=5.6, 2.0$ Hz, 1H, H6), 4.99 (sl, 1H, H_{18-PnM}), 4.31 (s, 1H, H1), 3.05 (s, 1H, H4), 2.78 (d, $J=2.1$ Hz, 1H, H3), 1.52–1.96 (m, 5 $H_{8-PnM}+H_{7syn}+H_{7anti}$), 1.45–1.50 (m, 1 H_{8-PnM}), 1.36 and 1.38 (2s, 6H, 8-(CH_3) $_2$ -8PnM), 0.87–1.52 (m, 2 H_{8-PnM}), 0.84 (d, $J=6.5$ Hz, 3H, 5- CH_3 -8PnM); ^{13}C NMR (100 MHz, $CDCl_3$): $\delta=171.5$ (COO), 149.3 (8- C_{ipso}), 138.0 (C5), 133.1 (C6), 128.0 ($2 \times C_{Ph}$), 126.0 ($2 \times C_{Ph}$), 125.0 (C_{para}), 72.6 (C_{18-PnM}), 70.8 (C3), 69.0 (C1), 51.3 (C_{28-PnM}), 47.2 (C4), 45.3 (C7), 39.8 (C_{8-PnM}), 39.7 (CH_2), 35.3 (CH_2), 26.0–27.1 ($C_{58-PnM}+2 \times 8-CH_3-8PnM$), 22.4 (CH_2), 22.1 (5- CH_3 -8PnM); ^{15}N NMR (40 MHz, $CDCl_3$): $\delta=150$.

4.6.4.6. Compound 10b. 1H NMR (400 MHz, $CDCl_3$): $\delta=7.27-7.35$ (m, 5 H_{Ph}), 7.17–7.24 (m, 1 H_{Ph}), 6.30 (dd, $J=5.5, 3.3$ Hz, 1H, H5), 6.21 (dd, $J=5.5, 2.5$ Hz, 1H, H6), 5.08 (br s, 1H, H_{18-PnM}), 4.16 (s, 1H, H1), 3.67 (d, $J=3.3$ Hz, 1H, H3), 3.28 (s, 1H, H4), 2.25 (d, $J=8.7$ Hz, 1H, H_{7syn}), 1.52–1.88 (m, 6 $H_{8-PnM}+H_{7anti}$), 1.33 and 1.34

(2s, 6H, 8-(CH_3) $_2$ -8PnM), 0.77–0.99 (m, 2 H_{8-PnM}), 0.82 (d, $J=6.6$ Hz, 3H, 5- CH_3 -8PnM).

4.6.4.7. Compound 11b. 1H NMR (400 MHz, $CDCl_3$): $\delta=7.26-7.35$ (m, 5 H_{Ph}), 7.17–7.24 (m, 1 H_{Ph}), 6.05–6.10 (m, 1H, H8), 5.55 (ddd, $J=5.6, 4.4, 2.1$ Hz, 1H, H7), 5.41–5.45 (m, 1H, H1), 5.32–5.50 (br s, 1H, NH), 5.05–5.08 (s, 1H, H_{18-PnM}), 3.88 (d, $J=7.9$ Hz, 1H, H4), 3.33–3.41 (m, 1H, H5), 2.38–2.47 (m, 1H, H_{6syn}), 2.12 (dq, $J=18.1, 2.3$ Hz, 1H, H_{6anti}), 1.88 (ddd, $J=14.4, 6.0, 3.6$ Hz, 1 H_{8-PnM}), 1.72–1.82 (m, 1 H_{8-PnM}), 1.46–1.70 (m, 4 H_{8-PnM}), 1.33 and 1.34 (2s, 6H, 8-(CH_3) $_2$ -8PnM), 0.96–1.10 (m, 2 H_{8-PnM}), 0.85 (d, $J=6.5$ Hz, 3H, 5- CH_3 -8PnM); ^{13}C NMR (100 MHz, $CDCl_3$): $\delta=168.5$ (COO), 148.9 (8- C_{ipso}), 137.6 (C8), 128.1 ($2 \times C_{Ph}$) and 126.0 ($2 \times C_{Ph}$), 126.0 (C7), 125.8 (C_{para}), 92.0 (C1), 72.4 (C_{18-PnM}), 67.4 (C4), 51.0 (C_{28-PnM}), 45.8 (C5), 39.9 (CH_2), 39.9 (C_{88-PnM}), 35.2 (CH_2), 34.2 (C6), 27.0 ($2 \times 8-CH_3-8PnM$), 26.0, 22.3 (CH_2), 21.9 (5- CH_3 -8PnM); ^{15}N NMR (40 MHz, $CDCl_3$): $\delta=141$; ESI-TOF: calculated for $[C_{23}H_{31}NO_3+H]^+$ ($M+H^+$) 370.23, found 370.2377.

4.6.4.8. Compound 11b'. 1H NMR (400 MHz, $CDCl_3$): $\delta=7.26-7.35$ (m, 5 H_{Ph}), 7.17–7.24 (m, 1 H_{Ph}), 6.10–6.14 (m, 1H, H8), 5.67 (ddd, $J=5.6, 4.4, 2.1$ Hz, 1H, H7), 5.44–5.48 (m, 1H, H1), 5.32–5.50 (br s, 1H, NH), 5.03–5.06 (s, 1H, H_{18-PnM}), 3.98 (d, $J=7.8$ Hz, 1H, H4), 3.41–3.49 (m, 1H, H5), 2.49–2.58 (m, 1H, H_{6syn}), 2.26 (dq, $J=18.1, 2.3$ Hz, 1H, H_{6anti}), 2.00 (ddd, $J=14.4, 6.0, 3.6$ Hz, 1 H_{8-PnM}), 1.72–1.82 (m, 1 H_{8-PnM}), 1.46–1.70 (m, 4 H_{8-PnM}), 1.33 and 1.34 (2s, 6H, 8-(CH_3) $_2$ -8PnM), 0.96–1.10 (m, 2 H_{8-PnM}), 0.84 (d, $J=6.5$ Hz, 3H, 5- CH_3 -8PnM); ^{13}C NMR (100 MHz, $CDCl_3$): $\delta=170.0$ (COO), 149.5 (8- C_{ipso}), 137.7 (C8), 128.0 ($2 \times C_{Ph}$) and 125.8 ($2 \times C_{Ph}$), 125.8 (C7), 125.8 (C_{para}), 92.0 (C1), 73.5 (C_{18-PnM}), 66.7 (C4), 50.9 (C_{28-PnM}), 45.8 (C5), 39.9 (C_{88-PnM}), 39.8 (CH_2), 35.3 (CH_2), 34.6 (C6), 26.9 ($2 \times 8-CH_3-8PnM$), 25.7, 22.3 (CH_2), 21.9; ^{15}N NMR (40 MHz, $CDCl_3$): $\delta=141$.

Acknowledgements

Thanks are due to Fundação para a Ciência e Tecnologia (FCT) for financial support through the re-equipment program REDE/1517/RMN/2005 and CONC-REEQ/275/QUI. C.A.D.S. acknowledges FCT for the award of the Research Grants SFRH/BD/31526/2006 and SFRH/BPD/80100/2011 and C.F.R.A.C.L. for the grant SFRH/BD/29394/2006.

Supplementary data

1H NMR and ^{13}C NMR spectra of all compounds plus NOE NMR data for 8-PMGO, 8-PnMGO and 8-PinMGO, as well as crystallographic data for 8-PnMGO and detailed computational results can be found. Supplementary data related to this article can be found online at <http://dx.doi.org/10.1016/j.tet.2013.03.033>. These data include MOL files and InChIKeys of the most important compounds described in this article.

References and notes

- (a) Corey, E. J.; Becker, K. B.; Varma, R. K. *J. Am. Chem. Soc.* **1972**, *94*, 8616–8618; (b) Corey, E. J.; Ensley, H. E. *J. Am. Chem. Soc.* **1975**, *97*, 6908–6909; (c) Quinkert, G.; Schmalz, H.; Dzierzynski, E. M.; Dürner, G.; Bats, J. W. *Angew. Chem., Int. Ed. Engl.* **1986**, *25*, 992–993; (d) Corey, E. J. *Angew. Chem., Int. Ed.* **2002**, *41*, 1650–1667.
- Whitesell, J. K.; Liu, C. L.; Buchanan, C. M.; Chen, H.-H.; Minton, M. A. J. *Org. Chem.* **1986**, *51*, 551–553.
- (a) Halterman, R. L.; Vollhard, K. P. C. *Organometallics* **1988**, *7*, 883–892; (b) Blanco, J. M.; Caamaño, O.; Fernández, F.; García-Mera, X.; López, C.; Rodríguez, G.; Rodríguez-Borges, J. E.; Rodríguez-Hergueta, *Tetrahedron Lett.* **1998**, *39*, 5663–5666; (c) Fernández, F.; García-Mera, X.; López, C.; Rodríguez, G.; Rodríguez-Borges, J. E. *Tetrahedron: Asymmetry* **2000**, *11*, 4805–4815; (d) Caamaño, O.; Fernández, F.; García-Mera, X.; Rodríguez-Borges, J. E. *Tetrahedron Lett.* **2000**, *41*, 4123–4125; (e) Fernández, F.; García-Mera, X.; Rodríguez-Borges, J. E.; Blanco, J. M. *Tetrahedron Lett.* **2001**, *42*, 5239–5240; (f) Fernández, F.; García-Mera, X.; Vale, M. L. C.; Rodríguez-Borges, J. E. *Synlett* **2005**, 319–321;

- (g) Vale, M. L. C.; Rodríguez-Borges, J. E.; Caamaño, O.; Fernández, F.; García-Mera, X. *Tetrahedron* **2006**, *62*, 9475–9482; (h) Xerardo García-Mera, X.; Rodríguez-Borges, J. E.; Vale, M. L.; Alves, M. J. *Tetrahedron* **2011**, *67*, 7162–7172.
4. (a) Binger, P.; Brinkmann, A.; Richter, W. *J. Tetrahedron Lett.* **1983**, *24*, 3599–3602; (b) Whitesell, J. K.; Bhattacharya, A. K.; Buchanan, C. M.; Chen, H.-H.; Deyo, D.; James, D.; Liu, C. L.; Minton, M. A. *Tetrahedron* **1986**, *42*, 2993–3001; (c) Fraile, J. M.; García, J. I.; Gracia, D.; Mayoral, J. A.; Pires, E. *J. Org. Chem.* **1996**, *61*, 9479–9482; (d) Takagi, R.; Kimura, J.; Shinohara, W.; Ohba, Y.; Takezono, K.; Hiraga, Y.; Kojima, S.; Ohkata, K. *J. Chem. Soc., Perkin Trans. 1* **1998**, 689–698; (e) Lerm, M.; Gais, H.-J.; Cheng, K.; Vermeeren, C. *J. Am. Chem. Soc.* **2003**, *125*, 9653–9667.
 5. Whitesell, J. K.; Bhattacharya, A. K.; Henke, K. *J. Chem. Soc., Chem. Commun.* **1982**, 988–989.
 6. Pascual-Teresa, B.; Gonzalez, J.; Asensio, A.; Houk, K. N. *J. Am. Chem. Soc.* **1995**, *117*, 4341–4356.
 7. Angelo, J.; Maddaluno, J. *J. Am. Chem. Soc.* **1986**, *108*, 8112–8114.
 8. (a) Sousa, C. A. D.; Vale, M. L. C.; Rodríguez-Borges, J. E.; García-Mera, X.; Rodríguez-Otero, J. *Tetrahedron Lett.* **2008**, *49*, 5777–5781; (b) Sousa, C. A. D.; Vale, M. L. C.; García-Mera, X.; Rodríguez-Borges, J. E. *Tetrahedron* **2012**, *68*, 1682–1687.
 9. Günther, H. *NMR Spectroscopy: Basic Principles, Concepts and Applications in Chemistry*, 2nd ed.; John Wiley: Chichester, UK and New York, NY, 1995, Chapter 4.
 10. Kleinspehn, G. G.; Jung, J. A.; Studniarz, S. A. *J. Org. Chem.* **1967**, *32*, 460–462.
 11. Grimme, S. *J. Chem. Phys.* **2003**, *118*, 9095–9102.
 12. (a) Lima, C. F. R. A. C.; Rocha, M. A. A.; Gomes, L. R.; Low, J. N.; Silva, A. M. S.; Santos, L. M. N. B. *F. Chem.—Eur. J.* **2012**, *18*, 8934–8943; (b) Lima, C. F. R. A. C.; Rocha, M. A. A.; Schröder, B.; Gomes, L. R.; Low, J. N.; Santos, L. M. N. B. *F. J. Phys. Chem. B* **2012**, *116*, 3557–3570.
 13. (a) Abramovich, M. A.; Ginzburg, I. M.; Ioffe, D. V. *Theor. Exp. Chem.* **1973**, *7*, 187–192; (b) Schwöbel, J.; Ebert, R.-U.; Kühne, R.; Schüürmann, G. *J. Chem. Inf. Model.* **2009**, *49*, 956–962.
 14. (a) Reeves, L. W.; Schneider, W. G. *Can. J. Chem.* **1957**, *35*, 251–261; (b) Tsuzuki, S. *Struct. Bonding (Berlin, Ger.)* **2005**, *115*, 149–193.
 15. The crystallographic data for the structure **4b** have been deposited at the Cambridge Crystallographic Data Center as supplementary publication number CCDC 787450. Copies of the data can be obtained free of charge on application to CCDC, 12 Union Road, Cambridge, CB2, 1EZ, UK.
 16. (a) Grigg, R.; Kemp, J.; Thompson, N. *Tetrahedron Lett.* **1978**, *31*, 2827–2830; (b) Grigg, R.; Jordan, M.; Tangthongkum, A. *J. Chem. Soc., Perkin Trans. 1* **1984**, 47–57; (c) Grigg, R. *Chem. Soc. Rev.* **1987**, *16*, 89–121; (d) Armstrong, P.; Grigg, R.; Surendrakumar, S.; Warnock, W. *J. Chem. Soc., Chem. Commun.* **1987**, 1327–1328.
 17. (a) Osborn, H. M. I.; Gemmill, N.; Harwood, L. M. *J. Chem. Soc., Perkin Trans. 1* **2002**, 2419–2438; (b) Mobinikhaledi, A.; Foroughifar, N.; Kalate, Z. *Turk. J. Chem.* **2005**, *29*, 147–152; (c) Hay, M. B.; Wolfe, J. P. *Angew. Chem., Int. Ed.* **2007**, *46*, 6492–6494.
 18. Romeo, G.; Iannazzo, D.; Piperno, A.; Romeo, R.; Corsaro, A.; Rescifina, A.; Chiacchio, U. *Mini-Rev. Org. Chem.* **2005**, *2*, 59–77.
 19. Palmer, G. C.; Ordy, M. J.; Simmons, R. D.; Strand, J. C.; Radov, L. A.; Mullen, G. B.; Kinsolving, C. R.; Georgiev, V. S.; Mitchell, J. T.; Allen, S. D. *Antimicrob. Agents Chemother.* **1989**, *33*, 895–905.
 20. Iannazzo, D. P. A.; Pistara, V.; Rescina, A.; Romeo, R. *Tetrahedron* **2002**, *58*, 581–587.
 21. (a) Chiacchio, U.; Rescifina, A.; Iannazzo, D.; Piperno, A.; Romeo, R.; Borrello, L.; Sciortino, M. T.; Balestrieri, E.; Macchi, B.; Mastino, A.; Romeo, G. *J. Med. Chem.* **2007**, *50*, 3747–3750; (b) Balestrieri, E.; Matteucci, C.; Ascolani, A.; Piperno, A.; Romeo, R.; Romeo, G.; Chiacchio, U.; Mastino, A.; Macchi, B. *Antimicrob. Agents Chemother.* **2008**, *52*, 54–64; (c) Loh, B.; Vozzolo, L.; Mok, B. J.; Lee, C. C.; Fitzmaurice, R. J.; Caddick, S.; Fassati, A. *Chem. Biol. Drug Des.* **2010**, *75*, 461–474.
 22. (a) Tamura, O.; Mitsuya, T.; Huang, X.; Tsutsumi, Y.; Hattori, S.; Ishibashi, H. *J. Org. Chem.* **2005**, *70*, 10720–10725; (b) Tamura, O.; Morita, N.; Takano, Y.; Fukui, K.; Okamoto, I.; Huang, X.; Tsutsumi, Y.; Ishibashi, H. *Synlett* **2007**, 658–660.
 23. (a) Ritson, D. J.; Cox, R. J.; Berge, J. *Org. Biomol. Chem.* **2004**, *2*, 1921–1933. (b) Sousa, C. A. D. Ph.D. Dissertation, Faculty of Sciences of University of Porto, Portugal, 2011.
 24. Frisch, M. J.; Trucks, G. W.; Schlegel, H. B.; Scuseria, G. E.; Robb, M. A.; Cheeseman, J. R.; Montgomery, J. A., Jr.; Vreven, T.; Kudin, K. N.; Burant, J. C.; Millam, J. M.; Iyengar, S. S.; Tomasi, J.; Barone, V.; Mennucci, B.; Cossi, M.; Scalmani, G.; Rega, N.; Petersson, G. A.; Nakatsuji, H.; Hada, M.; Ehara, M.; Toyota, K.; Fukuda, R.; Hasegawa, J.; Ishida, M.; Nakajima, T.; Honda, Y.; Kitao, O.; Nakai, H.; Klene, M.; Li, X.; Knox, J. E.; Hratchian, H. P.; Cross, J. B.; Bakken, V.; Adamo, C.; Jaramillo, J.; Gomperts, R.; Stratmann, R. E.; Yazyev, O.; Austin, A. J.; Cammi, R.; Pomelli, C.; Ochterski, J. W.; Ayala, P. Y.; Morokuma, K.; Voth, G. A.; Salvador, P.; Dannenberg, J. J.; Zakrzewski, V. G.; Dapprich, S.; Daniels, A. D.; Strain, M. C.; Farkas, O.; Malick, D. K.; Rabuck, A. D.; Raghavachari, K.; Foresman, J. B.; Ortiz, J. V.; Cui, Q.; Baboul, A. G.; Clifford, S.; Cioslowski, J.; Stefanov, B. B.; Liu, G.; Liashenko, A.; Piskorz, P.; Komaromi, I.; Martin, R. L.; Fox, D. J.; Keith, T.; Al-Laham, M. A.; Peng, C. Y.; Nanayakkara, A.; Challacombe, M.; Gill, P. M. W.; Johnson, B.; Chen, W.; Wong, M. W.; Gonzalez, C.; Pople, J. A. *Gaussian 03; Revision C.02*; Gaussian: Pittsburgh, PA, 2004.
 25. Bruker. *APEX2, SAINT and SADABS*; Bruker AXS: Madison, Wisconsin, USA, 2006.
 26. Altomare, A.; Casciarano, C.; Giacovazzo, C.; Guagliardi, A.; Moliterni, A. G. G.; Burla, M. C.; Polidori, G.; Camalli, M.; Spagna, R. *SIR97*; University of Bari: Italy, 1997.
 27. Sheldrick, G. M. *Acta Crystallogr.* **2008**, *A64*, 112–122.
 28. Farrugia, L. J. *J. Appl. Crystallogr.* **1997**, *30*, 565.
 29. Macrae, C. F.; Edgington, P. R.; McCabe, P.; Pidcock, E.; Shields, G. P.; Taylor, R.; Towler, M.; van de Streek, J. *J. Appl. Crystallogr.* **2006**, *39*, 453–457.
 30. Spek, A. L. *J. Appl. Crystallogr.* **2003**, *36*, 7–13.